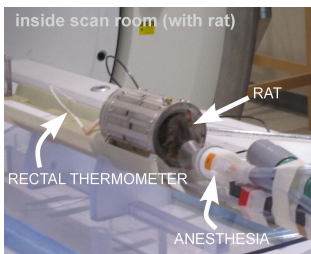


# Heat Induced Contrast Mechanisms in MRI: in vivo Tissue Characterization by MR Thermal Response

Matthew Tarasek<sup>1</sup>, Oguz Akin<sup>2</sup>, Jeannette Christine Roberts<sup>3</sup>, Tom Foo<sup>1</sup>, and Desmond T.B. Yeo<sup>1</sup>

<sup>1</sup>MRI, GE Global Research, Niskayuna, NY, United States, <sup>2</sup>Radiology, MSKCC, New York, NY, United States, <sup>3</sup>Imaging & Physiology Lab, GE Global Research, Niskayuna, NY, United States

**Purpose:** Clinical applications of Magnetic Resonance (MR) imaging in oncology has been rapidly evolving from being a subjective and interpretive diagnostic test based on tissue morphology to a more quantitative technique probing tissue biology [1]. MR imaging provides excellent spatial resolution and anatomical soft tissue contrast, yet there are still limitations in detecting and delineating early-stage cancer lesions when they are curable [2]. This is a major clinical impediment in cancer screening and therapy planning—even in the most common cancer types such as breast and prostate [3]. In hopes of extending ideas for a multiparametric, quantitative MRI data set, we evaluated a unique approach for MR contrast by utilizing the thermal responses of heat-sensitive MR parameters such as longitudinal relaxation time ( $T_1$ ), transverse relaxation time ( $T_2$ ), water proton chemical shift (CS), and apparent diffusion coefficient (ADC) [4-7]. We measure these thermally sensitive MR parameters at various temperatures to determine salient characteristics of *in vivo* tissue. We look for the accuracy and repeatability in measuring these parameters, and evaluate if heat-induced contrast mechanisms have the potential to add information to conventional MR imaging contrast types for better identification and characterization of tumors.



**Fig 1** Shows the general setup used for imaging / heating experiments, shown without oil vials or insulation

**Methods:** Our *in vivo* model included Fischer 344 rats injected with a breast adenocarcinoma cell line, Copenhagen rats injected with a rat prostate carcinoma cell line, and Sprague Dawley rats that have developed spontaneous benign mammary tumors. Rats were administered anesthesia and placed into a rat-sized transmit/receive quadrature Litz rat coil (Doty Scientific) as shown in Fig 1. The body temp of the rats were maintained at temps from ~20-40°C.  $T_1$  data sets were acquired using a 2D axial inversion recovery (IR) sequence at the following inversion time (TI) values: 3500, 2000, 950, 550, 350, 150, 50 with all times in ms. Other parameters included flip angle ( $\theta$ ) = 180°/90° set with proper TG, TR = 4500ms, TE = 4ms, freq FoV = 13cm, phase FoV = 6.5cm, matrix 128 x128, NEX = 1, 5 slices, 3-4 mm slice thickness.  $T_2$  data sets were acquired using a 2D axial spin echo (SE) sequence with the following TE values: 300, 150, 100, 125, 50, 25 and 4 ms,  $\theta$  = 90°/180° (set with proper TG), and same parameters as the IR experiments. ADC data sets were acquired from diffusion weighted images (DWI) using a 2D axial spin echo (SE) sequence with echo-planar imaging (EPI) readout at multiple b-values of 300-1200 s/mm<sup>2</sup>, and other parameters the same as the  $T_2$  images.

Fig 2a illustrates the data processing algorithm on a single slice example. Here 18 ROIs of ~38x38 voxels were taken at each inversion time (TI = 150 ms in Fig 2a) and  $T_1$  plots were made for each ROI. This procedure was repeated for a 3-5 slice acquisition giving typically 60-80  $T_1$  measurements (depending on the number of ROIs) to be used for averaging and standard deviation calculation. A similar approach was used for measuring  $T_2$  and ADC, allowing for the formation of distribution plots for all tumor and muscle tissue types. MR

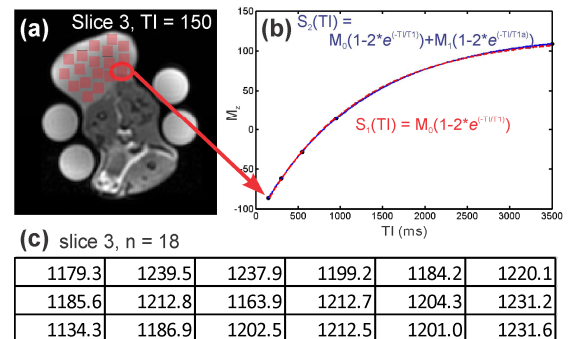


**Fig 2** Depiction of data processing algorithm. (a) Axial inversion-recovery image (TI = 150ms) through the center of malignant breast tumor. Average signal intensity in each ROI makes one point in a  $T_1$  plot similar to (b). (c) Shows the calculated  $T_1$  values for each ROI.

thermometry (MRT) was used during temp transition periods to (i) assess the apparent heating rate in different tissue structures and (ii) ensure that steady-state temps were achieved before relaxation parameter measurement. A 3-echo spoiled gradient echo (SPGR) imaging sequence ( $TE_1 \sim 5$ ms,  $TE_2 \sim 8$ ms,  $TE_3 \sim 11$ ms, TR=75ms,  $\theta=20^\circ$ , FoV=(13x6.5)cm<sup>2</sup>, matrix size=(128x128), 3x7mm slice acquisition) was used to perform MRT measurements. **Results:** For all animal models, we found a statistically significant difference ( $p < 0.05$ ) between quantitative contrast measurements for all tumor/muscle pairs. Percent change of thermal MR parameters  $\Gamma$  ( $\Gamma = T_1, T_2, ADC$ ) was measured as a function of temp ( $\% \Delta \Gamma / ^\circ C$ ). Calculations were made using the equation  $\% \Delta \Gamma / ^\circ C = ((\Gamma_{highT} - \Gamma_{lowT}) / \Gamma_{lowT}) / \Delta ^\circ C \times 100\%$  where  $\Gamma_{highT}$  is the high temp measure of  $\Gamma$ , and  $\Gamma_{lowT}$  is the low temp measure. A Student's t test was performed to determine statistically significant differences ( $p < 0.05$ ) between tumor and muscle for each thermal parameter  $\% \Delta \Gamma / ^\circ C$ . Results are summarized in Fig 3.

**Conclusions:** Most notably, we found significant difference in  $\% \Delta T_1 / ^\circ C$  and  $\% \Delta ADC / ^\circ C$  for the malignant breast adenocarcinoma compared to its surrounding muscle, along with a significant difference in  $\% \Delta T_2 / ^\circ C$  for the prostate carcinoma compared to its surrounding muscle tissue. These

findings indicate a link to a new method for improved MR imaging visualization/characterization of tissue with heat-induced contrast types. Specifically, the thermal responses of conventional MR imaging contrast mechanisms in different tissue types may contain new information for improved (i) delineation of tumor/tissue boundaries for diagnostic and therapy purposes, and (ii) characterization of salient characteristics for cancer diagnosis, e.g., malignant versus benign tumors. **References:** [1] Gillies et al. JMRI 2002;16:430, [2] Wu et al. Radiology 2009;2:253, [3] Mountford et al. Chem Rev 2004;104:3677, [4] Bloembergen et al. Phys Rev 1948;73:33, [5] Parker DL IEEE/BME 1984;31:161-7, [6] Riecke et al. JMRI 2008;27:376-90, [7] Chenevert et al. JMRI 2011;34:983-7